
Jean-Philippe Lansberg · Hua-Sheng Shao

Towards an automated tool to evaluate the impact of the nuclear modification of the gluon density on quarkonium, D and B meson production in proton-nucleus collisions

Abstract We propose a simple and model-independent procedure to account for the impact of the nuclear modification of the gluon density as encoded in nuclear collinear PDF sets on two-to-two partonic hard processes in proton-nucleus collisions. This applies to a good approximation to quarkonium, D and B meson production, generically referred to \mathcal{H} . Our procedure consists in parametrising the square of the parton scattering amplitude, $\mathcal{A}_{gg \rightarrow \mathcal{H}X}$ and constraining it from the proton-proton data. Doing so, we have been able to compute the corresponding nuclear modification factors for J/ψ , Υ and D^0 as a function of y and P_T at $\sqrt{s_{NN}} = 5$ and 8 TeV in the kinematics of the various LHC experiments in a model independent way. It is of course justified since the most important ingredient in such evaluations is the probability of each kinematical configuration. Our computations for D mesons can also be extended to B meson production. To further illustrate the potentiality of the tool, we provide –for the first time– predictions for the nuclear modification factor for η_c production in p Pb collisions at the LHC.

Keywords J/ψ , Υ , D , B , η_c production · heavy-ion collisions · nuclear PDFs · LHC

1 Introduction

For many years, open and closed heavy-flavour production in hadron-hadron, hadron-nucleus and nucleus-nucleus collisions has been a major subject of investigations, on both experimental and theoretical sides (see [1] for a review in the context of the first LHC results and [2, 3, 4, 5, 6] for earlier reviews). In addition of helping us to understand the interface between the perturbative and non-perturbative regimes of QCD in hadron-hadron collisions, these reactions are also sensitive to –and thus probe– the properties of the possible deconfined state of matter (QGP) resulting from nucleus-nucleus (AA) collisions at ultra-relativistic energies.

Yet, heavy-flavour production can also be affected by other nuclear effects¹ which are not related to a phase transition; they should in principle be subtracted in a way or another to study the QGP. These are typically believed to be the only ones acting in proton/deuteron-nucleus (pA) collisions at fixed-target, RHIC and LHC energies. Experimental results from RHIC and the LHC in pA collisions [1] have shown that the yields and the spectra of J/ψ , Υ , D and B are indeed modified in a magnitude which cannot simply be ignored in QGP studies. Many effects can be at play: break up within the nucleus [7, 8] or with comovers for the quarkonia [9, 10, 11, 12], coherent or incoherent energy loss [13, 14, 15, 16, 17], colour filtering [18], saturation/small- x /coherence effects [19, 20, 21, 22, 23], and the modification of the parton fluxes, as encoded in nuclear Parton Distribution Functions (nPDFs) [24, 25, 26, 27, 28].

In what follows, we will focus on the latter effects as a baseline for comparisons with experimental data. Our aim here is not to argue that it is indeed the dominant effect at RHIC and the LHC. Yet, a couple of recent

Jean-Philippe Lansberg
IPNO, Université Paris-Saclay, Univ. Paris-Sud, CNRS/IN2P3, F-91406, Orsay, France

Hua-Sheng Shao
Theoretical Physics Department, CERN, CH-1211 Geneva 23, Switzerland

¹ In what follows, we will call them “cold nuclear matter effects”.

comparisons [29, 1, 30] have shown that the magnitude of the gluon modification in usual nPDF fits is in reasonable agreement with quarkonium, D and B meson data in $p\text{Pb}$ collisions at the LHC.

nPDF fits are constantly updated with new data, recently from the LHC, and we have found it useful to propose a simple and model-independent procedure to account for the nPDF impact, in the particular case of gluon-induced $2 \rightarrow 2$ reactions². Such a procedure, to be encoded in a user friendly forthcoming tool, would then allow anybody to make up one's mind about the typical expected magnitude of the gluon nuclear modifications on a given probe.

In the past, shortcut procedures using simplified kinematics (like the one Drell-Yan at LO, that is $2 \rightarrow 1$) have widely been used [31, 32, 33, 34, 35]. However, it has been shown [36, 37, 38] that it can yield to systematics differences and, in principle, it cannot account for the P_T dependence of the yield. In general, it is just better to rely on a more proper $2 \rightarrow 2$ kinematics, although some higher QCD corrections could involve more than 2 hard particles in the final state at large P_T . For this purpose, a probabilistic Glauber Monte Carlo code, JIN [36, 37, 38], dedicated to the quarkonium case, has been developed to account for the geometry of the nuclear collisions and the impact parameter dependence of the nuclear effects at play along with the nPDF effect with an exact kinematics. However, as for now, the code deals with a limited number of processes (including though b production [39]) and of nPDFs; a simpler tool focusing on a $2 \rightarrow 2$ kinematics as the one we propose here is therefore very complementary. Eventually, both tools could interfaced or merged.

As will be explained below, the tool which we propose is based on HELAC-ONIA [40, 41] (but is not restricted to quarkonia) can use any nPDF set included in the library LHAPDF5 [42, 43] and LHAPDF6 [44] and does not rely on any model for the hard-probe production, but on pp measurements which are used to tune the partonic scattering elements.

2 Our approach

As announced, our approach is based on a data-driven modelling of the scattering at the partonic level. Once folded with proton PDFs, they yield pp cross sections and, when folded with one proton PDF and one nuclear PDF, they yield pA cross sections. Such a choice is essentially motivated by the case of inclusive quarkonium hadroproduction. Firstly, it makes the computations faster with a limited loss of generality. Secondly, we have to acknowledge that we do not have at present time a global and consistent theoretical description of inclusive quarkonium production in the whole transverse momentum domain at hadron colliders. Thirdly, most of available models on the market show uncertainties larger than those of the data which they are meant to describe (and which sometimes they do not). Some of these observation also apply to D and B production.

This translates into the following advantages:

1. one can describe single quarkonium, D and B production in pp collisions in a very satisfactory way with only 2 – 3 tuned parameters for each meson;
2. the uncertainty within our approach is well controlled by the available pp data which, as just said, is much smaller than the theoretical uncertainties of the state-of-the-art calculations;
3. the method is much more efficient to generate events, with significantly reduced Monte-Carlo uncertainty, owing to the simplicity of the computation.

2.1 pp cross section and partonic amplitude

As for the partonic scattering, we use a functional form for $|\overline{\mathcal{A}(k_1 k_2 \rightarrow \mathcal{H} + k_3)}|^2$ initially proposed in [45] and then successfully used in [46, 47, 48, 49] to model single quarkonium production at Tevatron and LHC energies in the context of double-parton scattering (DPS) studies. It reads

$$|\overline{\mathcal{A}(k_1 k_2 \rightarrow \mathcal{H} + k_3)}|^2 = \frac{\lambda^2 \kappa s x_1 x_2}{M_{\mathcal{H}}^2} \exp\left(-\kappa \frac{\min(P_T^2, \langle P_T \rangle^2)}{M_{\mathcal{H}}^2}\right) \left(1 + \theta(P_T^2 - \langle P_T \rangle^2) \frac{\kappa}{n} \frac{P_T^2 - \langle P_T \rangle^2}{M_Q^2}\right)^{-n}, \quad (1)$$

where k_i denote the partons involved in the hard scattering, $x_{1,2}$ are the momentum fractions carried by $k_{1,2}$, s is the square of the center-of-mass energy of the hadron collision, P_T ($M_{\mathcal{H}}$) is the transverse momentum (mass) of the produced particle, \mathcal{H} , and $\theta(x)$ is the Heaviside step function. $|\overline{\mathcal{A}}|^2$ is meant to account for the the

² We stress that a similar procedure could be devised for Drell-Yan pair, W and Z production.

squared amplitude averaged (summed) over the initial (final) helicity/colour factors. It contains 4 parameters $\lambda, \kappa, \langle P_T \rangle, n$, to be determined from the pp experimental data via a fit after the usual convolution with the PDFs:

$$\frac{d\sigma(pp \rightarrow \mathcal{H} + X)}{d\Phi_2} = \frac{1}{2s} \int dx_1 dx_2 x_1 f^p(x_1) x_2 f^p(x_2) \overline{|\mathcal{A}(k_1 k_2 \rightarrow Q + k_3)|^2}, \quad (2)$$

where f^p denotes the proton PDF and Φ_2 is the relativistic two-body phase space measure for the $2 \rightarrow 2$ scattering.

In what follows, we will only consider processes which are dominated by gluon fusion at LHC energies. All the procedure can readily be generalised to other partonic initial states.

2.2 Accounting for the nuclear PDF impact

As announced, we will also only consider the nuclear modification of the PDF among the possible effects acting on quarkonia, D and B mesons. Such a restriction would probably not yield a good description of the quarkonium excited states [2], which we therefore do not discuss. Along the same lines, we will focus on the LHC regime where the nuclear absorption is likely negligible. It may not be so at RHIC and even less at fixed-target energies.

Whereas one could think that the proposed procedure can be used to evaluate the sole impact of the nPDF on the excited states or the ground states at lower energies, one may want to be careful that in presence of other significant effects, the impact of the nPDFs may be affected. A clear example is a b -dependent antishadowing, which would tend to generate more J/ψ in the center of the overlap zone, which then may have more chance to be broken up by the nuclear absorption than those produced in the periphery of the overlap zone. Yet, the procedure should give a right order of magnitude of the nPDF impact even if other effects are at play.

As it is customary, the yield of a particle \mathcal{H} in pA collisions is obtained from that corresponding to the simple superposition of the equivalent number of pp collisions corrected by a factor encoding the nuclear modification of the parton flux. This is absolutely equivalent to directly using nuclear PDFs (normalised to the nucleus atomic number A) instead of proton PDFs. As aforementioned, our procedure does not currently rely on a Glauber code and we will thus restrict our studies to minimum bias collisions, *i.e.* integrated on all possible impact parameters b .

As such, the correction factor can be expressed in terms of the ratios R_i^A of the nuclear PDF (nPDF) in a nucleon belonging to a nucleus A to the PDF in the free nucleon:

$$R_i^A(x, Q^2) = \frac{f_i^A(x, Q^2)}{A f_i^p(x, Q^2)}, \quad i = q, \bar{q}, g. \quad (3)$$

To illustrate the potentiality of our procedure, we will only use two of the most up-to-date nPDF parameterisations resulting from global analyses with uncertainties. The first is EPS09 [27], which provides the fit uncertainties at both leading order (LO, dubbed EPS09LO) and next-to-leading order (NLO, dubbed EPS09NLO) and is available in the library LHAPDF5 [42]. The nPDF effects are given in terms of $R_i^A(x, Q^2)$ for all the flavours.

A new set, nCTEQ15 [24], has recently been released. It is available in the library LHAPDF6 [44] and provides NLO nuclear PDFs. As such, it is important to use the very same proton PDF as the one used for the fit. We have thus used CT14NLO [50]. In the case of EPS09, which provides ratios, the proton PDF to be used is less critical. In principle, we should have used CTEQ6(L1 or M) by consistency with EPS09, or CT14NLO for a good comparison of the yields with nCTEQ. Since CT14NLO is not available in LHAPDF5 and the code cannot load two PDF libraries at a time, we have preferred to use CT10NLO [51] which anyhow yields very similar gluon PDFs.

3 Fitting the LHC pp cross sections

At the LHC, we can essentially divide the inclusive (prompt) J/ψ production cross-sections measurements into 2 classes: the slightly forward and low P_T (from 0 up to roughly 20 GeV) data of LHCb and ALICE

and those from ATLAS and CMS at "high" P_T (from 6–8 up to roughly 100 GeV)³. We have performed 2 times $2\chi^2$ fits of $d^2\sigma/dP_T dy$ of prompt J/ψ production in pp collisions with 2 PDF sets (CT14NLO and CT10LO) using, on the one hand, LHCb data [52, 53] and, on the other, ATLAS [54] and CMS [55] data. The fit parameters ($\lambda, \kappa, \langle P_T \rangle$) and n of Eq. 1) are shown in Table. 1. A comparison of our fit results with the experimental data is shown in Fig. 1 (a) – (d). The procedure is particularly successful, but for a few marginal bins⁴. These will nevertheless do not have a visible impact on the pA observables to be discussed later.

PDF	data	λ	κ	$\langle P_T \rangle$	n
CT14NLO	LHCb [52, 53]	0.296 ± 0.118	0.558	4.5 (fixed)	2 (fixed)
	ATLAS [54] & CMS [55]	0.378	0.743 ± 0.0395	4.5 (fixed)	2 (fixed)
CT10NLO	LHCb [52, 53]	0.297	0.532	4.5 (fixed)	2 (fixed)
	ATLAS [54] & CMS [55]	0.383	0.750 ± 0.0364	4.5 (fixed)	2 (fixed)

Table 1: Results of a fit of $d^2\sigma/dP_T dy$ of prompt J/ψ in pp collisions using CT10NLO and CT14NLO, where we have fixed the values of n and $\langle P_T \rangle$. [The uncertainties from the χ^2 fit below the per cent level are not shown.]

PDF	λ	κ	$\langle P_T \rangle$	n
CT14NLO	0.768	0.0841 ± 0.0271	13.5 (fixed)	2 (fixed)
CT10NLO	0.687 ± 0.367	0.0864	13.5 (fixed)	2 (fixed)

Table 2: Results of a fit of $d^2\sigma/dP_T dy$ of inclusive $\Upsilon(1S)$ in pp collisions using CT10NLO and CT14NLO, where we have fixed the values of n and $\langle P_T \rangle$. The experimental data used in the fit are from ALICE [56], LHCb [57, 58], ATLAS [59] and CMS [60]. [The uncertainties from the χ^2 fit below the per cent level are not shown.]

PDF	λ	κ	$\langle P_T \rangle$	n
CT14NLO	0.558	0.398	4.5 (fixed)	2 (fixed)
CT10NLO	0.337	0.291	4.5 (fixed)	2 (fixed)

Table 3: Results of a fit of $d^2\sigma/dP_T dy$ of prompt $\eta_c(1S)$ in pp collisions using CT10NLO and CT14NLO, where we have fixed the values of n and $\langle P_T \rangle$. The experimental data used in the fit are from LHCb [61]. [The uncertainties from the χ^2 fit below the per cent level are not shown.]

PDF	λ	κ	$\langle P_T \rangle$	n
CT14NLO	2.29	1.11	0.88	2 (fixed)
CT10NLO	2.38	1.62	0.521	2 (fixed)

Table 4: Results of a fit of $d^2\sigma/dP_T dy$ of prompt D^0 in pp collisions using CT10NLO and CT14NLO, where the value of n was fixed. The experimental data used in the fit are from LHCb [62]. [The uncertainties from the χ^2 fit below the per cent level are not shown.]

For the $\Upsilon(1S)$ case, all the experiments have access to low P_T data and there is no b feed-down contamination. We have performed 2 fits (with CT14NLO and CT10LO) using data from ALICE [56], LHCb [57, 58], ATLAS [59] and CMS [60] altogether. See Table. 2 for the fit results and Fig. 1e–h for comparison with the fit spectra.

For the prompt η_c case, we have performed 2 fits (with CT14NLO and CT10LO) from the sole LHCb [61] data. See Table. 3 for the fit results and Fig. 1h for comparison with the fit spectra.

As for the D^0 , we have performed 2 fits (with CT14NLO and CT10LO) from the LHCb [62] data. See Table. 4 for the fit results and Fig. 1i for comparison with the fit spectra.

³ ALICE has also measured low P_T central J/ψ but with a limited statistical precision and a b feed-down contamination. The forward ALICE data are also prone to such a b feed-down contamination. As such, we will focus on the LHCb data for our fits in the forward and low P_T region. We also note that CMS has the capacity to cover P_T down to 3 GeV (even below in specific cases) in its most forward/backward acceptance.

⁴ Let us in particular note the slight discrepancy with the CMS very high P_T data. The very same fits are however consistent with the ATLAS data in the same P_T regime, which possibly indicates an underestimation of the systematical experimental uncertainties in that regime.

Just as for the J/ψ fits, the procedure works very well for $\Upsilon(1S)$, η_c and D^0 and gives us confidence that using the corresponding parametrised squared amplitudes will provide us with a reliable mapping of the $x_{1,2}$, y and P_T space.

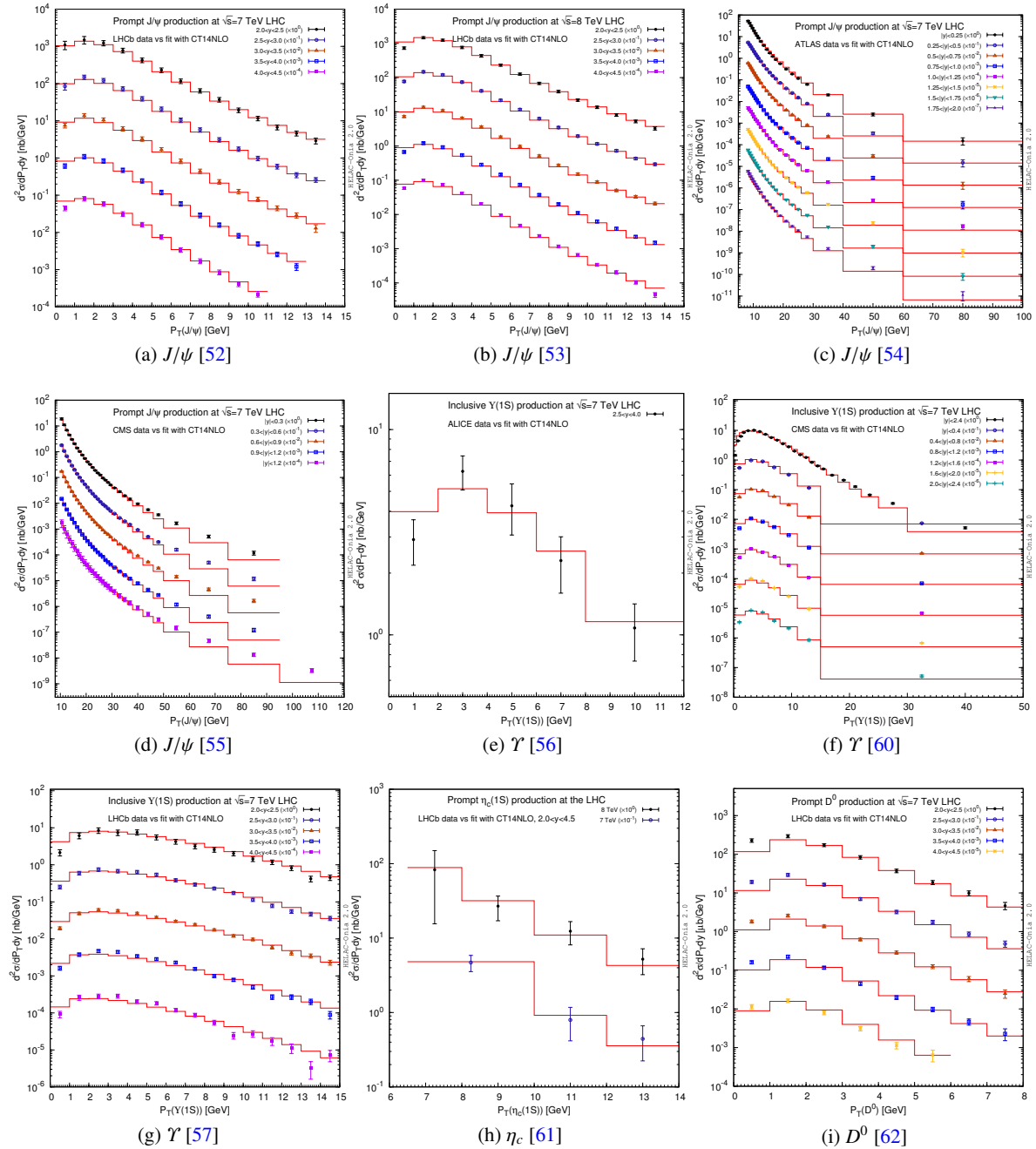


Fig. 1: Comparison of our fit results with the prompt J/ψ (a-d), inclusive Υ (e-g), prompt η_c (h) and prompt D^0 (i) production data in pp collisions at the LHC with CT14NLO as our proton PDF.

4 Results

4.1 Rapidity and transverse-momentum dependence of the production cross-section in $p\text{Pb}$ collisions at $\sqrt{s_{NN}} = 8 \text{ TeV}$

Now that we have described our approach, we can present our results for the cross-section for quarkonium and D^0 production in proton-lead ($p\text{Pb}$) collisions at the LHC. In the following, we show comparisons with all the existing data. As announced, we have employed three different nPDF EPS09LO, EPS09NLO and nCTEQ15. The sole nPDF uncertainties are displayed. In particular, we have not varied the factorisation scale despite the fact that it can indeed alter our results. Our histograms are calculated under the same cuts as the experimental data.

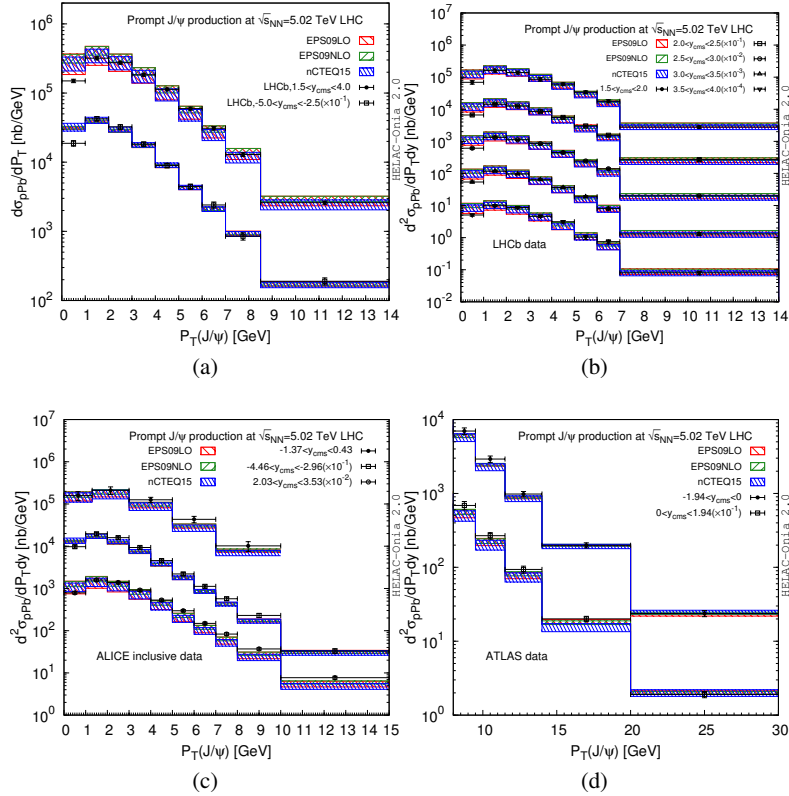


Fig. 2: Transverse-momentum dependence of the cross-section for prompt J/ψ production in $p\text{Pb}$ collisions at $\sqrt{s_{NN}} = 5.02 \text{ TeV}$: comparison between our results and the measurements of LHCb [63], ALICE [64] and ATLAS [65]. [The uncertainty bands represent the nuclear PDF uncertainty only].

The transverse-momentum P_T spectra ($d\sigma_{p\text{Pb}}/dP_T$) of promptly produced J/ψ in $p\text{Pb}$ collisions at $\sqrt{s_{NN}} = 5.02 \text{ TeV}$ are shown in Fig. 2. Comparisons are made with the LHCb prompt J/ψ production data [63] in both the forward ($1.5 < y_{\text{c.m.s.}} < 4.0$)⁵ and backward ($-5.0 < y_{\text{c.m.s.}} < -2.5$) rapidity regions in Fig. 2a. Fig. 2b shows a comparison with the double differential cross sections $d^2\sigma_{p\text{Pb}}/dP_T dy$ of J/ψ production of LHCb. Similarly, comparisons with the ALICE data [64] and ATLAS data [65] are given in Fig. 2c and Fig. 2d respectively. We note that ALICE data do not exclude the contribution from b -hadron decays. In general, the agreement with the yields differential in $P_T^{J/\psi}$ is satisfactory both at low P_T and high P_T .

⁵ Unless indicated, all rapidity y (or $y_{\text{c.m.s.}}$) mean the rapidity in the center-of-mass frame of nucleon-nucleon collision. In particular, rapidities in the laboratory frame would read y_{lab} .

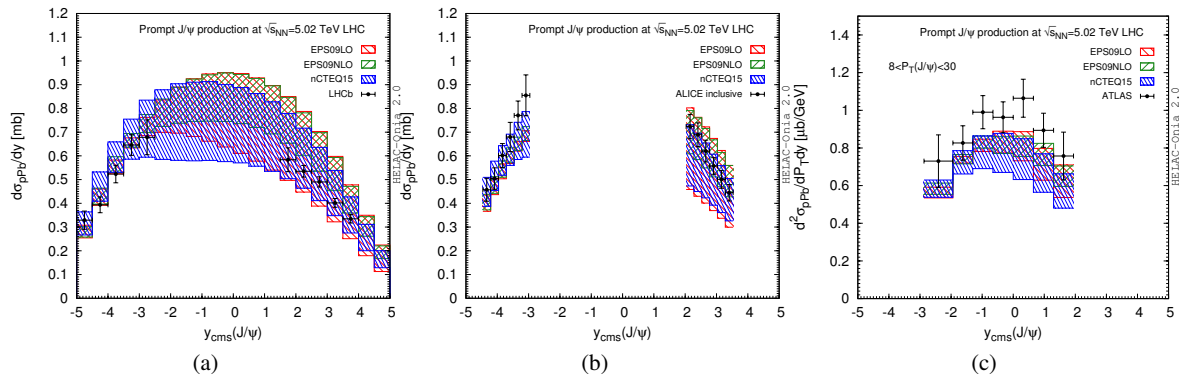


Fig. 3: Rapidity dependence of the cross-section for prompt J/ψ production in $p\text{Pb}$ collisions at $\sqrt{s_{NN}} = 5.02$ TeV: comparison between our results and the measurements of LHCb [63], ALICE [66] and ATLAS [65].

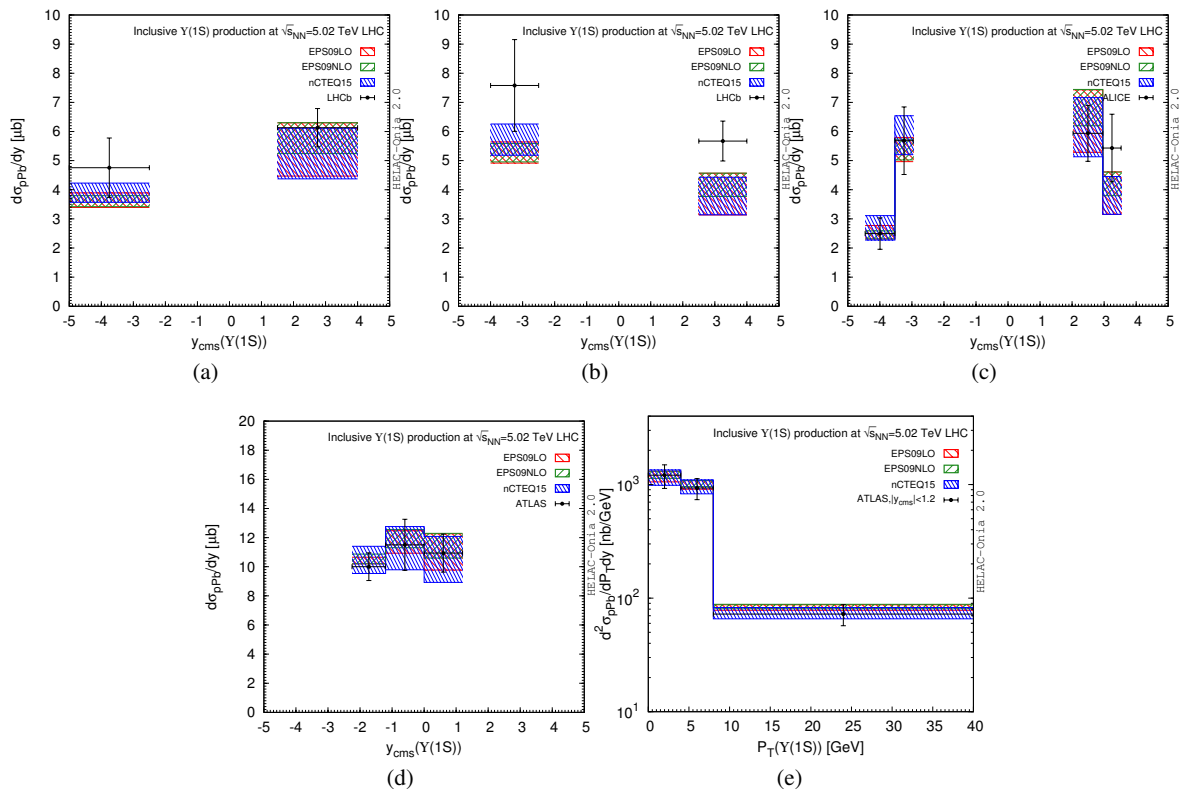


Fig. 4: Differential cross-section for inclusive $\Upsilon(1S)$ production in $p\text{Pb}$ collisions at $\sqrt{s_{NN}} = 5.02$ TeV: comparison of (a-d) the rapidity dependence obtained with our procedure with the measurements by LHCb [67], ALICE [68] and ATLAS [69] and (e) the transverse-momentum dependence as measured by ATLAS [69].

In Fig. 3, we have compared the LHCb [63], ALICE [66] and ATLAS data [65] with the J/ψ cross-section differential in y . It is interesting to notice that the results with the three nPDF show different uncertainties. In the forward region (low x_2), the result with EPS09NLO has the smallest uncertainty and tend to overshoot

the LHCb data [63] (see Fig. 3a). Such a discrepancy does not appear in Fig. 3b. One can also note that the EPS09LO uncertainty can be considered as the combination of both EPS09NLO and nCTEQ15 uncertainties in the forward region. In the backward region, owing to both the significant experimental and nPDF uncertainties, the three nPDFs are compatible with the data. At high P_T (in Fig. 3c for the ATLAS data [65]), although the central values of the experimental data are systematically higher than our theoretical bands, they remain compatible within one standard deviation. There could indeed be an overestimation of the nPDF suppression in this region or an offset in the ATLAS data.

As for the $\Upsilon(1S)$, Fig. 4a and 4b show comparisons with the LHCb data. The agreement is better when the full LHCb range is considered as opposed to that when the LHCb acceptance is restricted to a range where equal positive and negative y can be accessed (Fig. 4b). A good agreement is also obtained with the ALICE data (Fig. 4c) in a similar rapidity domain. In the ATLAS acceptance, all three nPDF magnitudes correctly account for the yield differential in y and P_T (Fig. 4d and 4e).

Fig. 5 and Fig. 6 show comparisons for the D^0 case between our results and the LHCb and ALICE measurements. The agreement is overall good. The yields tend to lie on the upper half of the uncertainty band. The nPDF uncertainties are however larger than for the quarkonia owing to the smaller value of the factorisation scale. As for the discrepancy in the first P_T bin of Fig. 5, one should be careful that our pp parametrisation is not optimal to describe it as well (see Fig. 1i) and tend to undershoot the pp yield.

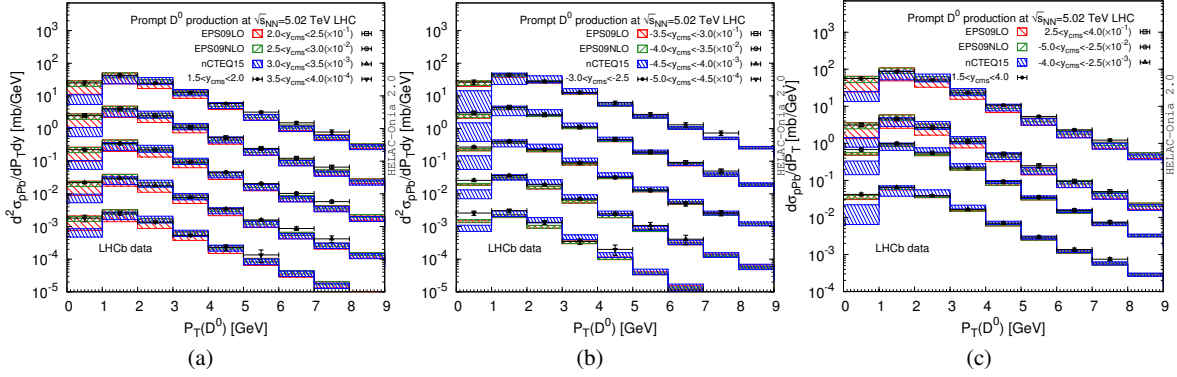


Fig. 5: Transverse-momentum dependence of the production cross-section of promptly produced D^0 in $p\text{Pb}$ collisions at $\sqrt{s_{NN}} = 5.02$ TeV: comparison between our results and the measurements by LHCb [70].

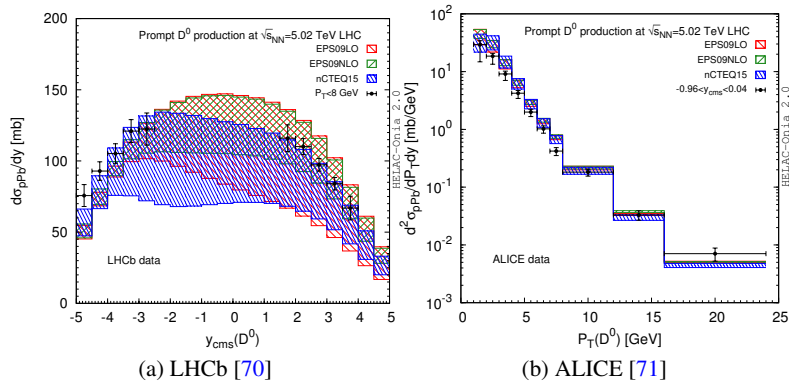


Fig. 6: (a) Rapidity [(b) Transverse-momentum] dependence of the cross-section for promptly produced D^0 in $p\text{Pb}$ at $\sqrt{s_{NN}} = 5.02$ TeV: comparison between our results and the measurements by LHCb [70] [ALICE [71]].

Finally, Fig. 7 show predictions –the first ever in the literature– for the P_T and y differential yield of η_c in the LHCb acceptance.

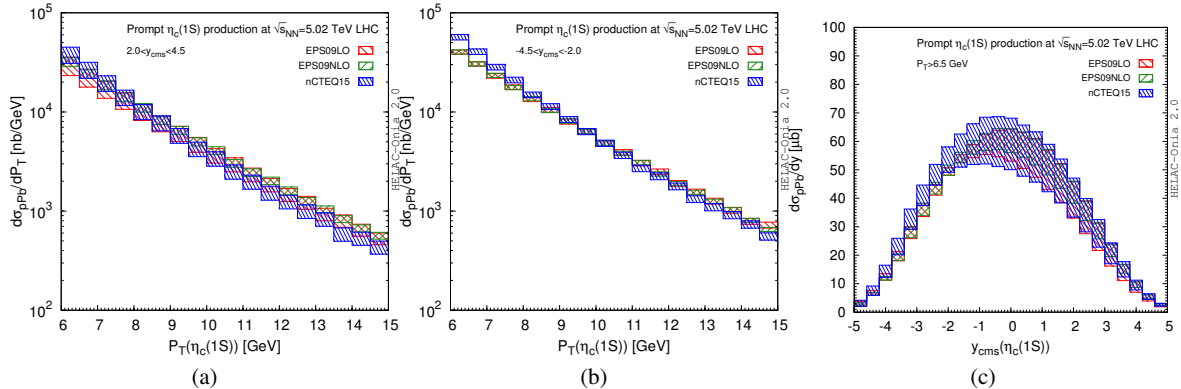


Fig. 7: (a-b) Transverse-momentum ((c) rapidity) dependence of the production cross-section of prompt $\eta_c(1S)$ in pPb collisions at $\sqrt{s_{NN}} = 5.02$ TeV. [The uncertainty bands represent the nuclear PDF uncertainty only.].

4.2 Rapidity and transverse-momentum dependence of R_{pPb} at $\sqrt{s_{NN}} = 5.02$ TeV

We now present and discuss our results for the *nuclear modification factor* R_{pPb} which characterises the yield modification of a given probe, say \mathcal{H} , in pPb collisions relative to pp collisions. It is the ratio obtained by normalising the \mathcal{H} yield in pPb collisions to the \mathcal{H} yield in pp collisions in the same kinematical conditions (y , P_T , nucleon-nucleon energy, etc.) times the average number of binary inelastic nucleon-nucleon collisions. When minimum bias collisions are considered, that is when all the possible geometrical configurations are summed over, it simplifies to the ratio of cross sections corrected by the atomic number of the nucleus ($A = 208$ for Pb):

$$R_{pPb} = \frac{d\sigma_{pPb}^{\mathcal{H}}}{Ad\sigma_{pp}^{\mathcal{H}}}. \quad (4)$$

We first discuss the rapidity dependence of R_{pPb} at the LHC with $\sqrt{s_{NN}} = 5.02$ TeV for J/ψ production. Our results obtained for the three nPDFs, EPS09LO, EPS09NLO and nCTEQ15 with their associated uncertainties are compared in Fig. 8 to the different experiments. Fig. 8a and Fig. 8b show low P_T data [63, 66, 64]. It is expected that the suppression in the forward region is due to the shadowing effect, while the enhancement in the backward region is due to the anti-shadowing effect. The experimental data are compatible with these expectations. Among the three different nPDFs, the data tend to favour the result obtained with nCTEQ15.

It is also interesting to note that the precision of the current data is already better than the nPDF uncertainties, especially in the forward region. This gives some hope that these measurements could ultimately be used to constrain the gluon density in heavy ions, provided that the impact of other nuclear effects could be disentangled. We also note that the shaded boxes on the right of the first two plots refer to the global systematical uncertainty. Such an information is not available for the ATLAS data. A good agreement with the LHCb and ALICE data is obtained; a slight discrepancy with the ATLAS data is observed. It is not clear whether it could be attributed to an offset in the data normalisation. In Fig. 9, we show further comparisons of R_{pPb} vs $P_T^{J/\psi}$ between our curves and the ALICE [64] and ATLAS [72] data. Similar to the rapidity distribution, a slight discrepancy is observed in Fig. 9b.

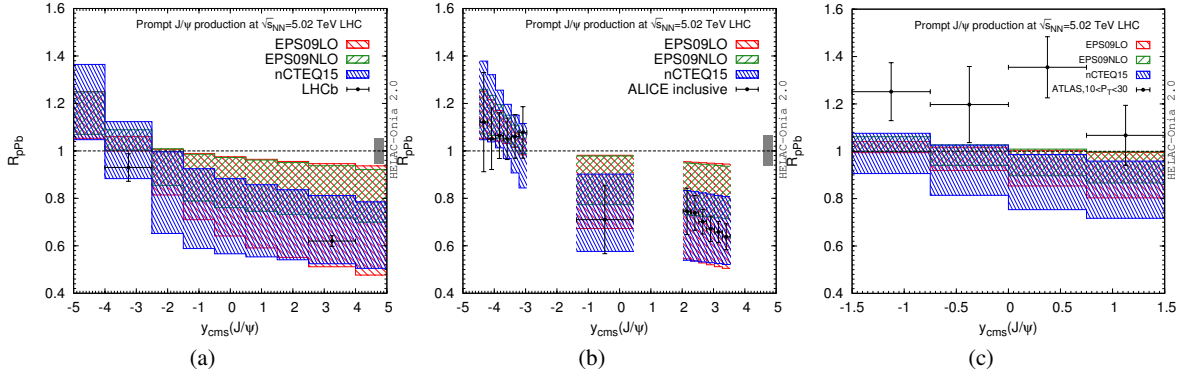


Fig. 8: Rapidity dependence of R_{pPb} of prompt J/ψ in pPb collisions at $\sqrt{s_{NN}} = 5.02$ TeV: comparison between our results and the measurements by LHCb [63], ALICE [66, 64] and ATLAS [72].

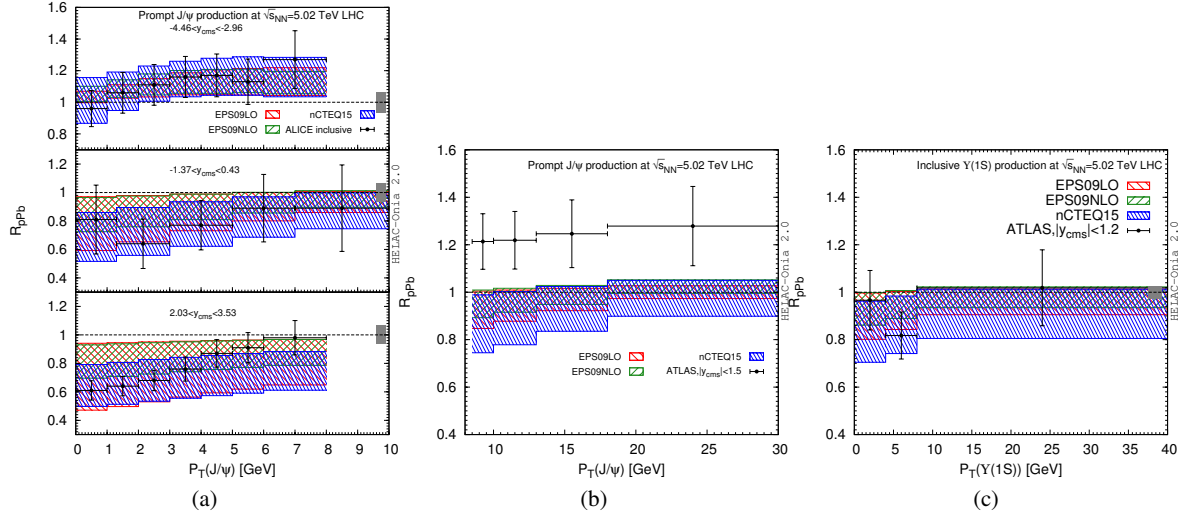


Fig. 9: (a-b) [(c)] P_T dependence of R_{pPb} of prompt J/ψ [inclusive $\Upsilon(1S)$] in pPb collisions at $\sqrt{s_{NN}} = 5.02$ TeV : comparison between our results and the measurements by ALICE [64] and ATLAS [72] [ATLAS [69]].

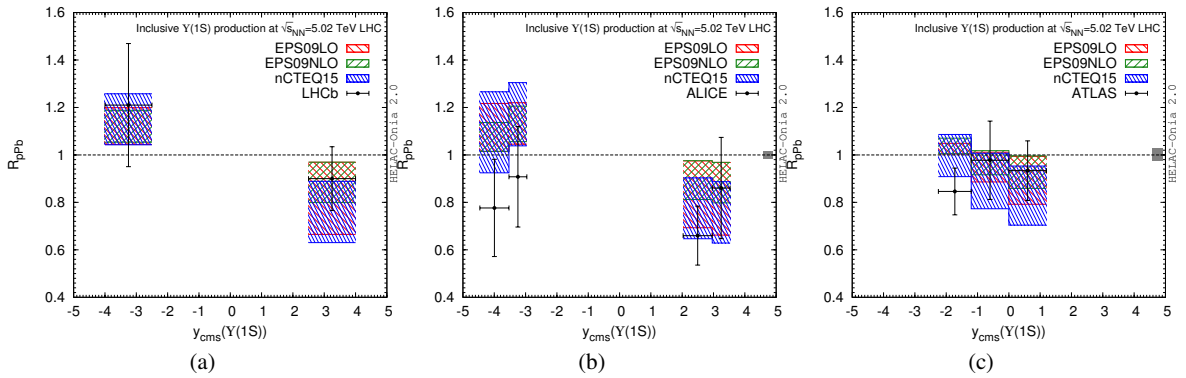


Fig. 10: Rapidity dependence of R_{pPb} of inclusive $\Upsilon(1S)$ in pPb collisions at $\sqrt{s_{NN}} = 5.02$ TeV: comparison between our results and the measurements by LHCb [67], ALICE [68] and ATLAS [69].

Similar comparisons are shown for $\mathcal{Y}(1S)$ on Fig. 10 and 9c. The overall agreement is acceptable given the large nPDF and experimental uncertainties. Further comparisons with the D^0 results are presented on Fig. 11. The agreement is also satisfactory and seems to indicate that EPS09 NLO is providing the best predictions. We however postpone further conclusions to the discussion of the R_{FB} results which however do not necessarily confirm this observation. To complete this exhaustive list of comparisons, we present our predictions for R_{pPb} of η_c in the LHCb acceptance of its pp analysis on Fig. 12. We are hopeful that it will motivate the first ever experimental studies of η_c in pPb collisions at the LHC.

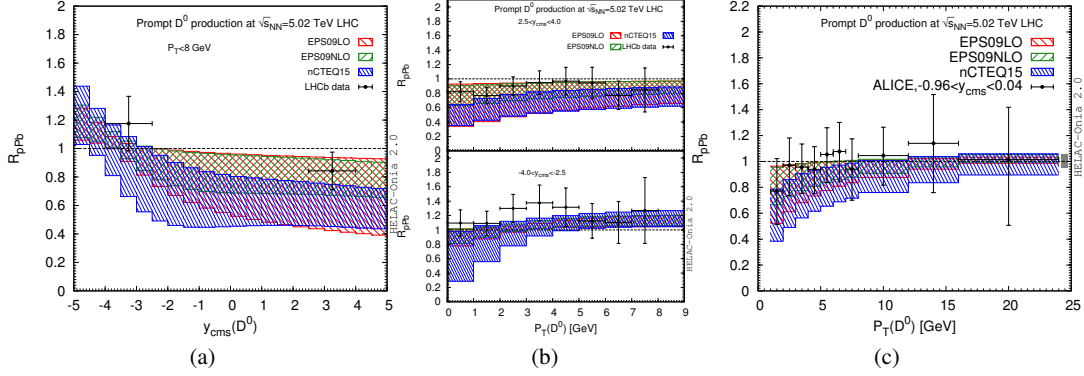


Fig. 11: Rapidity (a) and transverse-momentum (b-c) dependence of R_{pPb} of promptly produced D^0 in pPb collisions at $\sqrt{s_{NN}} = 5.02$ TeV: comparison between our results and the measurements by LHCb [70] (a-b) and ALICE [71] (c).

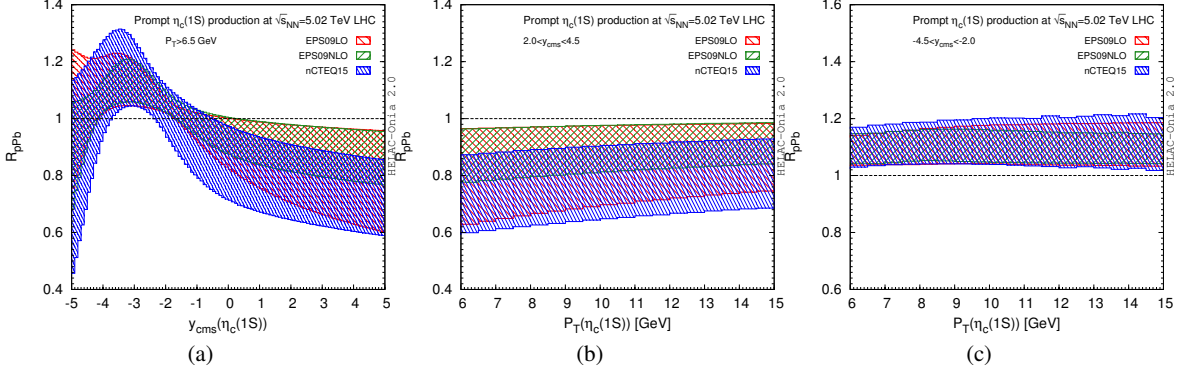


Fig. 12: Rapidity (a) and transverse-momentum (b-c) dependence of R_{pPb} of prompt $\eta_c(1S)$ in pPb collisions at $\sqrt{s_{NN}} = 5.02$ TeV.

4.3 Rapidity and transverse-momentum dependence of R_{FB} at $\sqrt{s_{NN}} = 5.02$ TeV

In this section, we discuss the forward-to-backward production ratio R_{FB} which results from the asymmetry of the proton-nucleus collision and is thus also sensitive to the nuclear effects. In addition, it has the advantage to be a ratio in which many of the systematic uncertainties of the data cancel, in particular that from the pp yield or cross section. It is defined as

$$R_{FB} = \frac{R_{pPb}(y_{c.m.s.} > 0)}{R_{pPb}(y_{c.m.s.} < 0)} = \frac{d\sigma_{pPb}^H(y_{c.m.s.} > 0)}{d\sigma_{pPb}^H(y_{c.m.s.} < 0)}, \quad (5)$$

where the "forward" direction was defined as the flight direction of the proton beam.

We stress that R_{FB} is identically unity at $y_{c.m.s.} = 0$. It tends to remain close to one if the nuclear effects cancel between the forward and backward regions, otherwise, it tends to increase more or less quickly for increasing $|y_{c.m.s.}|$. We further note that in the current implementation of our code the nPDF uncertainties in R_{FB} are generally smaller than in R_{pPb} (or in the cross sections). Indeed, our current code uses the same nPDF eigenset to compute the forward and the backward yields used in a given ratio. This amounts to consider that the uncertainties in the R_{pPb} are correlated. This interpretation (or rather use) of the information given by the nPDF is not unique and we could have considered that the nPDF uncertainties in R_{pPb} in the forward and backward regions are not necessarily correlated (as the widespread use of theory "bands" may suggest). Doing so, the uncertainties in R_{FB} would have been significantly larger. Finally, we recall that the global systematical uncertainties in the experimental data do cancel. On the experimental side, these results are usually much more reliable.

Fig. 13 displays our results for the rapidity dependence of R_{FB} for the three gluon nPDFs used before (EPS09LO, EPS09NLO, nCTEQ15). For the low P_T data of LHCb and ALICE, the magnitude of the asymmetry is well compatible with that of nCTEQ15 and EPS09 LO, at the lower edge of the EPS09 NLO range. As for the ATLAS data with a P_T cut, their current uncertainties and the reduced magnitude of the effects (since $|y_{c.m.s.}|$ is smaller) do not allow for any conclusions.

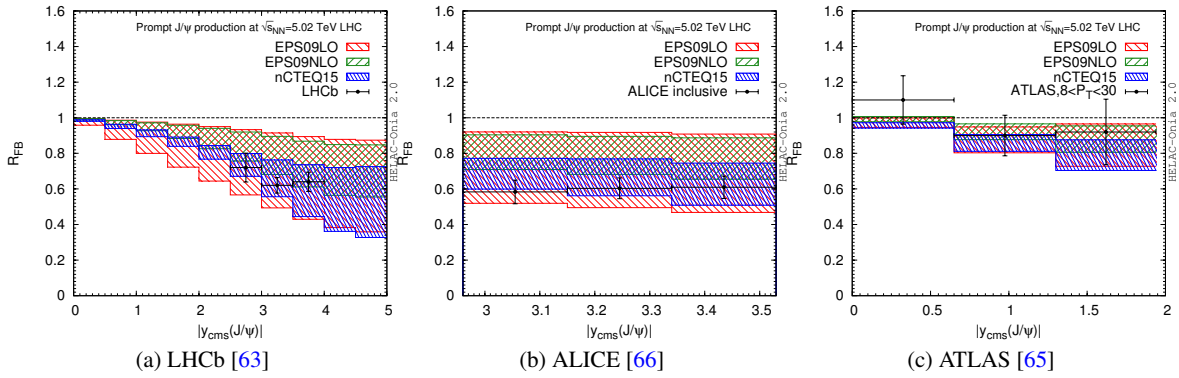


Fig. 13: Rapidity dependence of R_{FB} of J/ψ in pPb collisions at $\sqrt{s_{NN}} = 5.02$ TeV: comparison between our results and the measurements by LHCb [63], ALICE [66] and ATLAS [65]. [The uncertainty bands represent the nuclear PDF uncertainty only. ALICE data are for inclusive J/ψ .]

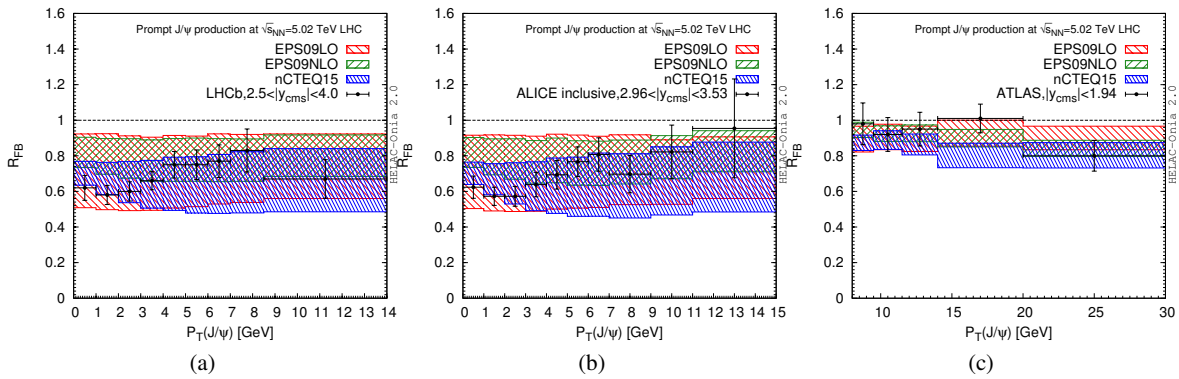


Fig. 14: Transverse-momentum dependence of the R_{FB} of J/ψ in pPb collisions at $\sqrt{s_{NN}} = 5.02$ TeV: comparison between our results and the LHCb [63], ALICE [66] and ATLAS [65] data.

Fig. 14 shows our results for R_{FB} versus $P_T^{J/\psi}$. A clear trend is seen in the LHCb and ALICE results with a ratio increasing with P_T , starting at 0.6. R_{FB} at P_T above 10 GeV are compatible with unity, but the larger

uncertainties do not exclude values smaller than one. The magnitude of the ratio in the data is compatible with the 3 nPDFs. More advanced studies are needed to go further in the interpretation of the P_T dependence using specific eigensets as opposed to bands. We also recall that a given nPDF set can be compatible with R_{FB} and not with R_{pPb} . This can happen due to specific cancellations in the magnitude of the forward and backward nuclear modifications or to a normalisation offset. In particular, we note that there is no tension at all with the ATLAS data for R_{FB} (Fig. 13c and Fig. 14c) unlike the case of R_{pPb} (Fig. 8c and Fig. 9b). We are inclined to attribute this to a normalisation offset from the pp baseline whose effect disappears in R_{FB} .

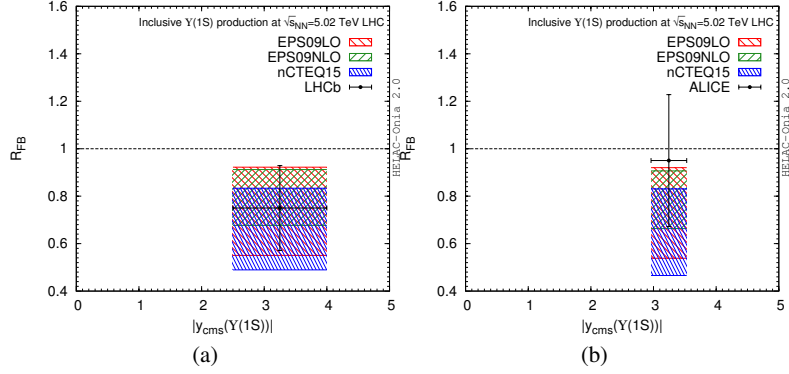


Fig. 15: Rapidity dependence of R_{FB} of inclusive $\Upsilon(1S)$ in pPb collisions at $\sqrt{s_{NN}} = 5.02$ TeV: comparison between our results and the measurements of LHCb [67] and ALICE [68].

We have also computed R_{FB} for $\Upsilon(1S)$ (Fig. 15) and D^0 (Fig. 16). The same remarks as for the J/ψ case apply. No tension between the data and our computation are found. Just as for the ATLAS J/ψ data, the good agreement with the D^0 LHCb data may indicate that a slight offset in the normalisation affects R_{pPb} as plotted on Fig. 11. Whereas the R_{pPb} values point at a smaller suppression than those encoded in the nPDFs (in particular nCTEQ15), the magnitude of R_{FB} is very well accounted by nCTEQ15 and corresponds to the strongest magnitude encoded in EPS09 NLO. For completeness, we have also computed R_{FB} of prompt $\eta_c(1S)$ (see Fig. 17).

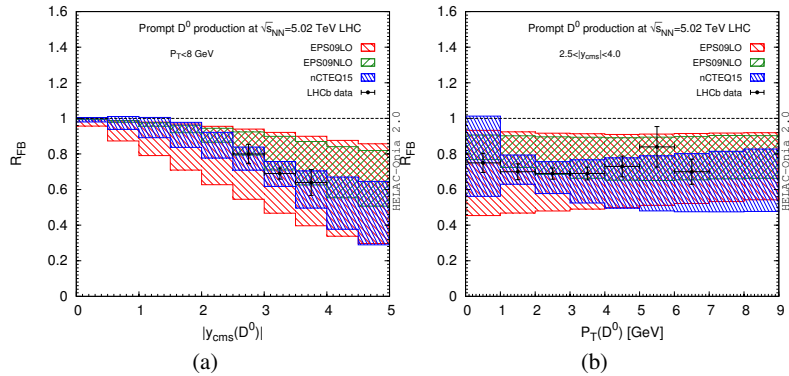


Fig. 16: Rapidity (a) and transverse-momentum (b) dependence of R_{FB} of prompt D^0 production in pPb collisions at $\sqrt{s_{NN}} = 5.02$ TeV: comparison between our results and the measurements by LHCb [70].

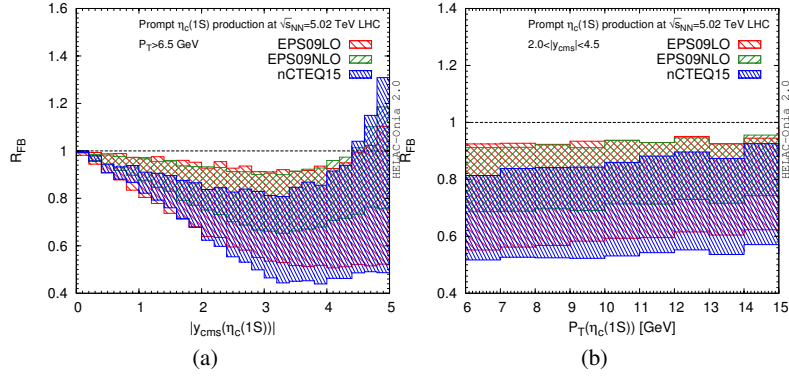


Fig. 17: Rapidity (a) and transverse-momentum (b) dependence of R_{FB} of prompt $\eta_c(1S)$ in $p\text{Pb}$ collisions at $\sqrt{s_{\text{NN}}} = 5.02$ TeV.

5 Conclusions

We have devised a model-independent procedure to evaluate the impact of the nuclear modification of the gluon densities on hard probes produced in proton-nucleus collisions at collider energies. It is particularly tailored for two-to-two partonic scatterings, relevant for quarkonium and heavy-meson production. The model independence of our procedure lies in the parametrisation of the partonic amplitude squared with parameters fit to pp collision data in similar kinematical conditions as the $p\text{Pb}$ data to be described.

We have illustrated the capabilities of our approach by computing the cross sections as well as the nuclear modifications factor for J/ψ , Υ and D^0 production at the LHC. Even though our objective was not to argue that the nPDF effect is the dominant one in this energy range, we have not found out any significant tension between our computations using three common nPDFs (EPS09 LO & NLO and nCTEQ15) and the existing data. To further highlight the potentialities of the approach, we have made predictions for η_c production which might be at reach for the LHCb collaboration. We have also made predictions for the 8 TeV $p\text{Pb}$ run (see the appendix).

As outlooks for physics studies, our method can easily be transposed to B hadron production. It should also be possible to apply it for non-prompt charmonia provided that the kinematical shift between the b -quark and the charmonium is correctly accounted for. On the side of the tool itself, we plan improve it such that it could automatically provide the user with the nuclear modification factors starting for measured pp data.

Acknowledgements

We are very grateful to R. Araldi, E.G. Ferreira, F. Fleuret, C. Hadjidakis, D. Kikola, Y. Kim, A. Kusina, S. Lee, A. Rakatozafindrabe, C. Salgado, I. Schienbein, R. Vogt, Z. Yang, Y. Zhang for stimulating discussions. The work of J.P.L. is supported in part by the French CNRS via the LIA FCPPL (Quarkonium4AFTER) and the Défi Inphyniti-Théorie LHC France. H.S.S. is supported by the ERC grant 291377 *LHCtheory: Theoretical predictions and analyses of LHC physics: advancing the precision frontier*.

References

1. A. Andronic *et al.*, “Heavy-flavour and quarkonium production in the LHC era: from proton-proton to heavy-ion collisions,” *Eur. Phys. J. C* **76** no. 3, (2016) 107, [arXiv:1506.03981 \[nucl-ex\]](#).
2. J. P. Lansberg, “Theory status of quarkonium production in proton-nucleus collisions,” *J. Phys. Conf. Ser.* **668** no. 1, (2016) 012019, [arXiv:1510.01818 \[nucl-th\]](#).
3. N. Brambilla *et al.*, “Heavy quarkonium: progress, puzzles, and opportunities,” *Eur. Phys. J. C* **71** (2011) 1534, [arXiv:1010.5827 \[hep-ph\]](#).
4. R. Rapp, D. Blaschke, and P. Crochet, “Charmonium and bottomonium production in heavy-ion collisions,” *Prog. Part. Nucl. Phys.* **65** (2010) 209–266, [arXiv:0807.2470 \[hep-ph\]](#).

5. A. D. Frawley, T. Ullrich, and R. Vogt, "Heavy flavor in heavy-ion collisions at RHIC and RHIC II," *Phys. Rept.* **462** (2008) 125–175, [arXiv:0806.1013 \[nucl-ex\]](#).
6. J. P. Lansberg, " J/ψ , ψ' and Υ production at hadron colliders: A Review," *Int. J. Mod. Phys.* **A21** (2006) 3857–3916, [arXiv:hep-ph/0602091 \[hep-ph\]](#).
7. C. Gerschel and J. Hufner, "A Contribution to the Suppression of the J/ψ Meson Produced in High-Energy Nucleus Nucleus Collisions," *Phys. Lett.* **B207** (1988) 253–256.
8. R. Vogt, " J/ψ production and suppression," *Phys. Rept.* **310** (1999) 197–260.
9. E. G. Ferreira, "Excited charmonium suppression in proton-nucleus collisions as a consequence of comovers," *Phys. Lett.* **B749** (2015) 98–103, [arXiv:1411.0549 \[hep-ph\]](#).
10. A. Capella and E. G. Ferreira, " J/ψ suppression at $s^{*}(1/2) = 200$ -GeV in the comovers interaction model," *Eur. Phys. J.* **C42** (2005) 419–424, [arXiv:hep-ph/0505032 \[hep-ph\]](#).
11. A. Capella, E. G. Ferreira, and A. B. Kaidalov, "Nonsaturation of the J/ψ suppression at large transverse energy in the comovers approach," *Phys. Rev. Lett.* **85** (2000) 2080–2083, [arXiv:hep-ph/0002300 \[hep-ph\]](#).
12. S. Gavin and R. Vogt, " J/ψ Suppression From Hadron - Nucleus to Nucleus-nucleus Collisions," *Nucl. Phys.* **B345** (1990) 104–124.
13. F. Arleo and S. Peigne, " J/ψ suppression in p-A collisions from parton energy loss in cold QCD matter," *Phys. Rev. Lett.* **109** (2012) 122301, [arXiv:1204.4609 \[hep-ph\]](#).
14. R. Sharma and I. Vitev, "High transverse momentum quarkonium production and dissociation in heavy ion collisions," *Phys. Rev.* **C87** no. 4, (2013) 044905, [arXiv:1203.0329 \[hep-ph\]](#).
15. F. Arleo, S. Peigne, and T. Sami, "Revisiting scaling properties of medium-induced gluon radiation," *Phys. Rev.* **D83** (2011) 114036, [arXiv:1006.0818 \[hep-ph\]](#).
16. S. J. Brodsky and P. Hoyer, "A Bound on the energy loss of partons in nuclei," *Phys. Lett.* **B298** (1993) 165–170, [arXiv:hep-ph/9210262 \[hep-ph\]](#).
17. S. Gavin and J. Milana, "Energy loss at large $x(F)$ in nuclear collisions," *Phys. Rev. Lett.* **68** (1992) 1834–1837.
18. S. J. Brodsky and P. Hoyer, "The Nucleus as a Color Filter in QCD Decays: Hadroproduction in Nuclei," *Phys. Rev. Lett.* **63** (1989) 1566.
19. B. Ducloué, T. Lappi, and H. Mantysaari, "Forward J/ψ production in proton-nucleus collisions at high energy," *Phys. Rev.* **D91** no. 11, (2015) 114005, [arXiv:1503.02789 \[hep-ph\]](#).
20. Y.-Q. Ma, R. Venugopalan, and H.-F. Zhang, " J/ψ production and suppression in high energy proton-nucleus collisions," *Phys. Rev.* **D92** (2015) 071901, [arXiv:1503.07772 \[hep-ph\]](#).
21. H. Fujii and K. Watanabe, "Heavy quark pair production in high energy pA collisions: Quarkonium," *Nucl. Phys.* **A915** (2013) 1–23, [arXiv:1304.2221 \[hep-ph\]](#).
22. J.-W. Qiu, P. Sun, B.-W. Xiao, and F. Yuan, "Universal Suppression of Heavy Quarkonium Production in pA Collisions at Low Transverse Momentum," *Phys. Rev.* **D89** no. 3, (2014) 034007, [arXiv:1310.2230 \[hep-ph\]](#).
23. B. Kopeliovich, A. Tarasov, and J. Hufner, "Coherence phenomena in charmonium production off nuclei at the energies of RHIC and LHC," *Nucl. Phys.* **A696** (2001) 669–714, [arXiv:hep-ph/0104256 \[hep-ph\]](#).
24. K. Kovarik *et al.*, "nCTEQ15 - Global analysis of nuclear parton distributions with uncertainties in the CTEQ framework," *Phys. Rev.* **D93** no. 8, (2016) 085037, [arXiv:1509.00792 \[hep-ph\]](#).
25. J. F. Owens, A. Accardi, and W. Melnitchouk, "Global parton distributions with nuclear and finite- Q^2 corrections," *Phys. Rev.* **D87** no. 9, (2013) 094012, [arXiv:1212.1702 \[hep-ph\]](#).
26. D. de Florian, R. Sassot, P. Zurita, and M. Stratmann, "Global Analysis of Nuclear Parton Distributions," *Phys. Rev.* **D85** (2012) 074028, [arXiv:1112.6324 \[hep-ph\]](#).
27. K. J. Eskola, H. Paukkunen, and C. A. Salgado, "EPS09: A New Generation of NLO and LO Nuclear Parton Distribution Functions," *JHEP* **04** (2009) 065, [arXiv:0902.4154 \[hep-ph\]](#).
28. M. Hirai, S. Kumano, and T. H. Nagai, "Determination of nuclear parton distribution functions and their uncertainties in next-to-leading order," *Phys. Rev.* **C76** (2007) 065207, [arXiv:0709.3038 \[hep-ph\]](#).
29. J. L. Albacete *et al.*, "Predictions for p+Pb Collisions at $\sqrt{s_{NN}} = 5$ TeV: Comparison with Data," *Int. J. Mod. Phys.* **E25** no. 09, (2016) 1630005, [arXiv:1605.09479 \[hep-ph\]](#).
30. E. G. Ferreira, F. Fleuret, J. P. Lansberg, and A. Rakotozafindrabe, "Impact of the Nuclear Modification of the Gluon Densities on J/ψ production in pPb collisions at $\sqrt{s_{NN}} = 5$ TeV," *Phys. Rev.* **C88** no. 4, (2013) 047901, [arXiv:1305.4569 \[hep-ph\]](#).
31. R. Vogt, "Shadowing and absorption effects on J/ψ production in dA collisions," *Phys. Rev.* **C71** (2005) 054902, [arXiv:hep-ph/0411378 \[hep-ph\]](#).
32. F. Arleo and V.-N. Tram, "A Systematic study of J/ψ suppression in cold nuclear matter," *Eur. Phys. J.* **C55** (2008) 449–461, [arXiv:hep-ph/0612043 \[hep-ph\]](#).
33. F. Arleo, "Constraints on nuclear gluon densities from J/ψ data," *Phys. Lett.* **B666** (2008) 31–33, [arXiv:0804.2802 \[hep-ph\]](#).
34. C. Lourenco, R. Vogt, and H. K. Woehri, "Energy dependence of J/ψ absorption in proton-nucleus collisions," *JHEP* **02** (2009) 014, [arXiv:0901.3054 \[hep-ph\]](#).
35. R. Vogt, "Cold Nuclear Matter Effects on J/ψ and Υ Production at the LHC," *Phys. Rev.* **C81** (2010) 044903, [arXiv:1003.3497 \[hep-ph\]](#).
36. E. G. Ferreira, F. Fleuret, and A. Rakotozafindrabe, "Transverse momentum dependence of J/ψ shadowing effects," *Eur. Phys. J.* **C61** (2009) 859–864, [arXiv:0801.4949 \[hep-ph\]](#).
37. E. G. Ferreira, F. Fleuret, J. P. Lansberg, and A. Rakotozafindrabe, "Cold nuclear matter effects on J/ψ production: Intrinsic and extrinsic transverse momentum effects," *Phys. Lett.* **B680** (2009) 50–55, [arXiv:0809.4684 \[hep-ph\]](#).
38. E. G. Ferreira, F. Fleuret, J. P. Lansberg, and A. Rakotozafindrabe, "Centrality, Rapidity and Transverse-Momentum Dependence of Cold Nuclear Matter Effects on J/ψ Production in d Au, Cu Cu and Au Au Collisions at $s(NN)^{*(1/2)} = 200$ -GeV," *Phys. Rev.* **C81** (2010) 064911, [arXiv:0912.4498 \[hep-ph\]](#).

-
39. Z. Conesa del Valle, E. G. Ferreiro, F. Fleuret, J. P. Lansberg, and A. Rakotozafindrabe, “Open-beauty production in $p\text{Pb}$ collisions at $\sqrt{s_{NN}}=5$ TeV: effect of the gluon nuclear densities,” [arXiv:1402.1747 \[hep-ph\]](#). [Nucl. Phys.A926,236(2014)].
40. H.-S. Shao, “HELAC-Onia: An automatic matrix element generator for heavy quarkonium physics,” *Comput. Phys. Commun.* **184** (2013) 2562–2570, [arXiv:1212.5293 \[hep-ph\]](#).
41. H.-S. Shao, “HELAC-Onia 2.0: an upgraded matrix-element and event generator for heavy quarkonium physics,” *Comput. Phys. Commun.* **198** (2016) 238–259, [arXiv:1507.03435 \[hep-ph\]](#).
42. M. R. Whalley, D. Bourilkov, and R. C. Group, “The Les Houches accord PDFs (LHAPDF) and LHAGLUE,” in *HERA and the LHC: A Workshop on the implications of HERA for LHC physics. Proceedings, Part B*. 2005. [arXiv:hep-ph/0508110 \[hep-ph\]](#).
43. D. Bourilkov, R. C. Group, and M. R. Whalley, “LHAPDF: PDF use from the Tevatron to the LHC,” in *TeV4LHC Workshop - 4th meeting Batavia, Illinois, October 20-22, 2005*. 2006. [arXiv:hep-ph/0605240 \[hep-ph\]](#).
44. A. Buckley, S. Lloyd, K. Nordström, B. Page, M. Rfenacht, M. Schnherr, and G. Watt, “LHAPDF6: parton density access in the LHC precision era,” *Eur. Phys. J. C* **75** (2015) 132, [arXiv:1412.7420 \[hep-ph\]](#).
45. C. H. Kom, A. Kulesza, and W. J. Stirling, “Pair Production of J/ψ as a Probe of Double Parton Scattering at LHCb,” *Phys. Rev. Lett.* **107** (2011) 082002, [arXiv:1105.4186 \[hep-ph\]](#).
46. J.-P. Lansberg and H.-S. Shao, “ J/ψ -pair production at large momenta: Indications for double parton scatterings and large α_s^2 contributions,” *Phys. Lett. B* **751** (2015) 479–486, [arXiv:1410.8822 \[hep-ph\]](#).
47. J.-P. Lansberg and H.-S. Shao, “Double-quarkonium production at a fixed-target experiment at the LHC (AFTER@LHC),” *Nucl. Phys. B* **900** (2015) 273–294, [arXiv:1504.06531 \[hep-ph\]](#).
48. H.-S. Shao and Y.-J. Zhang, “Complete study of hadroproduction of a Υ meson associated with a prompt J/ψ ,” *Phys. Rev. Lett.* **117** no. 6, (2016) 062001, [arXiv:1605.03061 \[hep-ph\]](#).
49. C. Borschensky and A. Kulesza, “Double parton scattering in pair-production of J/ψ mesons at the LHC revisited,” [arXiv:1610.00666 \[hep-ph\]](#).
50. S. Dulat, T.-J. Hou, J. Gao, M. Guzzi, J. Huston, P. Nadolsky, J. Pumplin, C. Schmidt, D. Stump, and C. P. Yuan, “New parton distribution functions from a global analysis of quantum chromodynamics,” *Phys. Rev. D* **93** no. 3, (2016) 033006, [arXiv:1506.07443 \[hep-ph\]](#).
51. H.-L. Lai, M. Guzzi, J. Huston, Z. Li, P. M. Nadolsky, J. Pumplin, and C. P. Yuan, “New parton distributions for collider physics,” *Phys. Rev. D* **82** (2010) 074024, [arXiv:1007.2241 \[hep-ph\]](#).
52. LHCb Collaboration, R. Aaij *et al.*, “Measurement of J/ψ production in pp collisions at $\sqrt{s} = 7$ TeV,” *Eur. Phys. J. C* **71** (2011) 1645, [arXiv:1103.0423 \[hep-ex\]](#).
53. LHCb Collaboration, R. Aaij *et al.*, “Production of J/ψ and Upsilon mesons in pp collisions at $\sqrt{s} = 8$ TeV,” *JHEP* **06** (2013) 064, [arXiv:1304.6977 \[hep-ex\]](#).
54. ATLAS Collaboration, G. Aad *et al.*, “Measurement of the differential cross-sections of prompt and non-prompt production of J/ψ and $\psi(2S)$ in pp collisions at $\sqrt{s} = 7$ and 8 TeV with the ATLAS detector,” *Eur. Phys. J. C* **76** no. 5, (2016) 283, [arXiv:1512.03657 \[hep-ex\]](#).
55. CMS Collaboration, V. Khachatryan *et al.*, “Measurement of J/ψ and $\psi(2S)$ Prompt Double-Differential Cross Sections in pp Collisions at $\sqrt{s}=7\text{TeV}$,” *Phys. Rev. Lett.* **114** no. 19, (2015) 191802, [arXiv:1502.04155 \[hep-ex\]](#).
56. ALICE Collaboration, B. B. Abelev *et al.*, “Measurement of quarkonium production at forward rapidity in pp collisions at $\sqrt{s} = 7$ TeV,” *Eur. Phys. J. C* **74** no. 8, (2014) 2974, [arXiv:1403.3648 \[nucl-ex\]](#).
57. LHCb Collaboration, R. Aaij *et al.*, “Measurement of Upsilon production in pp collisions at $\sqrt{s} = 7$ TeV,” *Eur. Phys. J. C* **72** (2012) 2025, [arXiv:1202.6579 \[hep-ex\]](#).
58. LHCb Collaboration, R. Aaij *et al.*, “Forward production of Υ mesons in pp collisions at $\sqrt{s} = 7$ and 8 TeV,” *JHEP* **11** (2015) 103, [arXiv:1509.02372 \[hep-ex\]](#).
59. ATLAS Collaboration, G. Aad *et al.*, “Measurement of Upsilon production in 7 TeV pp collisions at ATLAS,” *Phys. Rev. D* **87** no. 5, (2013) 052004, [arXiv:1211.7255 \[hep-ex\]](#).
60. CMS Collaboration, S. Chatrchyan *et al.*, “Measurement of the $\Upsilon(1S)$, $\Upsilon(2S)$, and $\Upsilon(3S)$ cross sections in pp collisions at $\sqrt{s} = 7$ TeV,” *Phys. Lett. B* **727** (2013) 101–125, [arXiv:1303.5900 \[hep-ex\]](#).
61. LHCb Collaboration, R. Aaij *et al.*, “Measurement of the $\eta_c(1S)$ production cross-section in proton-proton collisions via the decay $\eta_c(1S) \rightarrow p\bar{p}$,” *Eur. Phys. J. C* **75** no. 7, (2015) 311, [arXiv:1409.3612 \[hep-ex\]](#).
62. LHCb Collaboration, R. Aaij *et al.*, “Prompt charm production in pp collisions at $\sqrt{s}=7$ TeV,” *Nucl. Phys. B* **871** (2013) 1–20, [arXiv:1302.2864 \[hep-ex\]](#).
63. LHCb Collaboration, R. Aaij *et al.*, “Study of J/ψ production and cold nuclear matter effects in $p\text{Pb}$ collisions at $\sqrt{s_{NN}} = 5$ TeV,” *JHEP* **02** (2014) 072, [arXiv:1308.6729 \[nucl-ex\]](#).
64. ALICE Collaboration, J. Adam *et al.*, “Rapidity and transverse-momentum dependence of the inclusive J/ψ nuclear modification factor in $p\text{-Pb}$ collisions at $\sqrt{s_{NN}} = 5.02$ TeV,” *JHEP* **06** (2015) 055, [arXiv:1503.07179 \[nucl-ex\]](#).
65. ATLAS Collaboration, G. Aad *et al.*, “Measurement of differential J/ψ production cross sections and forward-backward ratios in $p\text{-Pb}$ collisions with the ATLAS detector,” *Phys. Rev. C* **92** no. 3, (2015) 034904, [arXiv:1505.08141 \[hep-ex\]](#).
66. ALICE Collaboration, B. B. Abelev *et al.*, “ J/ψ production and nuclear effects in $p\text{-Pb}$ collisions at $\sqrt{s_{NN}} = 5.02$ TeV,” *JHEP* **02** (2014) 073, [arXiv:1308.6726 \[nucl-ex\]](#).
67. LHCb Collaboration, R. Aaij *et al.*, “Study of Υ production and cold nuclear matter effects in $p\text{Pb}$ collisions at $\sqrt{s_{NN}}=5$ TeV,” *JHEP* **07** (2014) 094, [arXiv:1405.5152 \[nucl-ex\]](#).
68. ALICE Collaboration, B. B. Abelev *et al.*, “Production of inclusive $\Upsilon(1S)$ and $\Upsilon(2S)$ in $p\text{-Pb}$ collisions at $\sqrt{s_{NN}} = 5.02$ TeV,” *Phys. Lett. B* **740** (2015) 105–117, [arXiv:1410.2234 \[nucl-ex\]](#).
69. ATLAS Collaboration, “Measurement of $\Upsilon(nS)$ production with $p\text{-Pb}$ collisions at $\sqrt{s_{NN}} = 5.02$ TeV and pp collisions at $\sqrt{s} = 2.76$ TeV,” Tech. Rep. ATLAS-CONF-2015-050, CERN, Geneva, Sep, 2015. <https://cds.cern.ch/record/2055266>.

-
70. **LHCb** Collaboration, “Study of cold nuclear matter effects using prompt D^0 meson production in p Pb collisions at LHCb,” Tech. Rep. LHCb-CONF-2016-003, CERN, Geneva, Mar, 2016. <http://cds.cern.ch/record/2138946>.
 71. **ALICE** Collaboration, B. B. Abelev *et al.*, “Measurement of prompt D -meson production in $p - Pb$ collisions at $\sqrt{s_{NN}} = 5.02$ TeV,” *Phys. Rev. Lett.* **113** no. 23, (2014) 232301, [arXiv:1405.3452](https://arxiv.org/abs/1405.3452) [nucl-ex].
 72. **ATLAS** Collaboration, T. A. collaboration, “Study of J/ψ and $\psi(2S)$ production in $\sqrt{s_{NN}} = 5.02$ TeV $p + Pb$ and $\sqrt{s} = 2.76$ TeV pp collisions with the ATLAS detector,” Tech. Rep. ATLAS-CONF-2015-023, 2015.

A Appendix: Predictions for the p Pb run at 8 TeV.

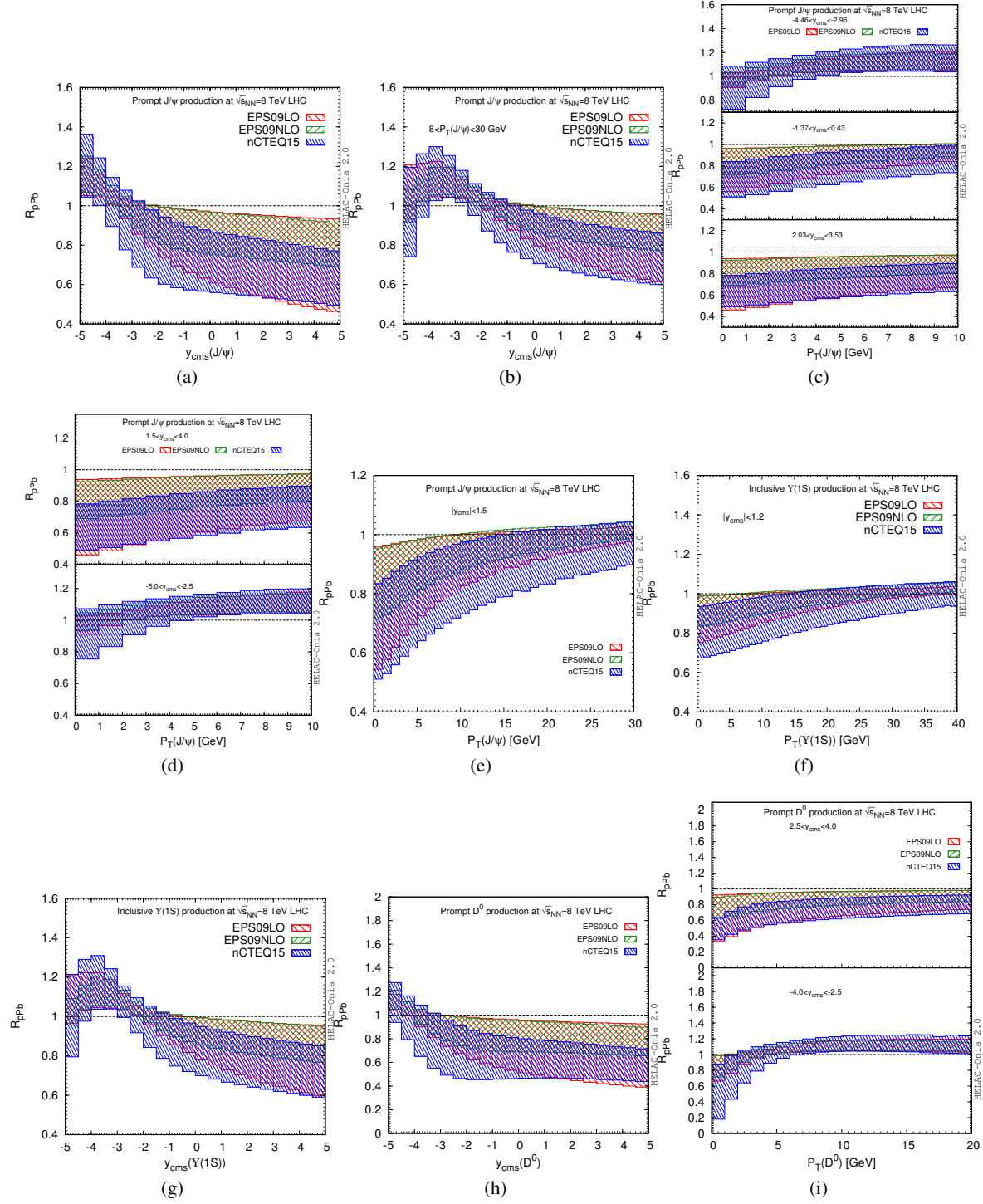


Fig. 18: Predictions for 8 TeV in different rapidity and transverse momentum regions.